Satellite evidence of substantial rain-induced soil emissions of ammonia across the Sahel

Jonathan E. Hickman[1, *], Enrico Dammers[2], Corinne Galy-Lacaux[3], Guido R. Van der Werf[1]

5 [1]Earth and Climate Cluster, Vrije Universiteit, Amsterdam, 1081 HV, Netherlands

[2]Environment and Climate Change Canada, Toronto, Ontario, M3H 5T4, Canada

[3]Laboratoire d'Aérologie UPS-CNRS UMR 5560, Toulouse, 31400, France

*now at NASA Goddard Institute for Space Studies, New York, NY, 10025, USA

Correspondence to: Jonathan E. Hickman (jonathan.e.hickman@nasa.gov)

10 **Abstract.** Atmospheric ammonia (NH_3) is a precursor to fine particulate matter formation and contributes to nitrogen deposition, with potential implications for the health of humans and ecosystems. Agricultural soils and animal excreta are the primary source of atmospheric NH_3, but natural soils can also be an important emittor. In regions with distinct dry and wet seasons such as the Sahel, the start of the rainy season triggers a pulse of biogeochemical activity in surface soils known as the Birch effect,

15 which is often accompanied by emissions of microbially-produced gases such as carbon dioxide and nitric oxide. Field and lab studies have sometimes, but not always, observed pulses of NH_3 after the wetting of dry soils; however, the potential regional importance of these emissions remains poorly constrained. Here we use satellite retrievals of atmospheric NH_3 using the Infrared Atmospheric Sounding Interferometer (IASI) regridded at 0.25° resolution, in combination with satellite-based

20 observations of precipitation, surface soil moisture, and nitric dioxide concentrations, to present evidence of substantial precipitation-induced pulses of NH_3 across the Sahel at the onset of the rainy season in 2008. The highest concentrations of NH_3 occur in pulses during March and April, when biomass burning emissions estimated for the region by the Global Fire Emissions Database database are low. For the region of the Sahel spanning 10° to 16° N and 0° to 30° E, changes in NH_3 concentrations

25 are weakly but significantly correlated with changes in soil moisture during the period from mid-March through April, when the peak NH_3 concentrations occur (r=0.28, p=0.02). The correlation is also present

when evaluated on an individual pixel-basis during April (r=0.16, p<0.001). Using a simple box model, average emissions for the entire Sahel are between 2 and 6 mg NH_3 m^{-2} day^{-1} during peaks of the observed pulses, depending on the assumed effective lifetime. These early season pulses are consistent with surface observations of monthly deposition, which show an uptick in NH_3 deposition at the start of

5   the rainy season for sites in the Sahel. The NH_3 concentrations in April are also correlated with increasing tropospheric NO_2 concentrations observed by the Ozone Monitoring Instrument (r=0.78, p<0.0001), which have previously been attributed to the Birch effect. Box model results suggest that pulses occurring over a 35-day period in March and April are responsible for roughly one fifth of annual NH_3 emissions from the Sahel. We conclude that precipitation early in the rainy season is responsible

10 for substantial NH_3 emissions in the Sahel, likely representing the largest instantaneous fluxes of nitrogen gas from the region during the year.

1. Introduction

Ammonia (NH_3) plays an important role in the atmosphere and in the nitrogen (N) cycle. In the atmosphere, NH_3 is a precursor to the formation of fine particular matter ($PM_{2.5}$), which contributes to

15 substantial levels of premature mortality (Lelieveld et al., 2015). (NH_3) can also form a substantial proportion of atmospheric N deposition (Dentener et al., 2006; Holland et al., 2005), affecting downwind ecosystems by potentially altering productivity (Thomas et al., 2009), soil pH (Tian and Niu, 2015), eutrophication status (Bergstrom and Jannson, 2006), biodiversity (Bobbink et al., 2010), and stimulating emissions of other trace gases such as nitric oxide (NO) and nitrous oxide (N_2O; e.g.,

20 (Eickenscheidt et al., 2011; Pilegaard et al., 2006).

Cropland and grazed soils have long been known to be a major source of atmospheric ammonia through the volatilization of urea and ammonium (NH_4^+) based inorganic fertilizers as well as of livestock excreta (Bouwman et al., 1997). Ammonia emissions can also represent an important N flux in

25 natural ecosystems, particularly in drylands. In deserts, soil NH_3 emissions can represent over 25% of

annual nitrogen losses (McCalley and Sparks, 2008) and over 10% in a semiarid savanna (Fiona M Soper, 2016).

Soil moisture is a key control over biogeochemical cycles in drylands (Austin et al., 2004).
5 Biogeochemical cycling in dryland soils is often characterized by pulsing dynamics related to the wetting or re-wetting of dry soils, known as the Birch effect (Birch, 1960; Birch and Friend, 1956). In environments where the distribution of annual precipitation is distinctly seasonal, soil microbial activity typically declines during the dry season, as water becomes limiting and microbes senesce or become dormant (Borken and Matzner, 2009). N may build up in soils during this period, when little biological
10 uptake occurs, but when atmospheric N deposition continues and senesced microbial and plant material accumulates (Borken and Matzner, 2009). The onset of the rainy season can initiate a rapid increase in microbial activity (Birch and Friend, 1956; Borken and Matzner, 2009; Placella and Firestone, 2013; Placella et al., 2012), as re-awakened microbes take advantage of pools of N that accumulated or were made more bioavailable during the dry season, leading to large increases in N mineralization rates
15 (Birch, 1958; 1960; Borken and Matzner, 2009; Dijkstra et al., 2012; Saetre and Stark, 2004; Semb and Robinson, 1969).

The abrupt change in water potential also represents a stress to microbes, prompting a flush of labile N solutes released by microbes to maintain turgor pressure (Kieft et al., 1987). This increase in
20 microbial activity is accompanied by pulsed emissions of trace gases such as carbon dioxide (CO_2; Emmerich, 2003; Huxman et al., 2004; Saetre and Stark, 2004) and NO (e.g., Anderson and Levine, 1986; Davidson, 1992), which can be an important component of annual emissions (Davidson, 1992; Jaeglé et al., 2004). As the availability of NH_4^+ is a major control over NH_3 volatilization (Nelson, 1982; Schlesinger and Peterjohn, 1991), a flush of N mineralization would be expected to trigger an
25 NH_3 emission pulse as well. A few studies have documented pulse dynamics in emissions of NH_3 in laboratory or field settings (Delon et al., 2017; McCalley and Sparks, 2008; Schlesinger and Peterjohn, 1991; Soper et al., 2016). In arid and semi-arid ecosystems, soil NH_3 emissions have been observed to increase by ~15% to 630% (Schlesinger and Peterjohn, 1991), though there are few studies outside

desert ecosystems (Kim et al., 2012), and an increase in NH_3 emissions following wetting is not always observed (e.g., Yahdjian and Sala, 2010). The potential importance of these pulse emissions of NH_3 at landscape or regional scales remains poorly constrained.

5   In addition to NH_4^+ availability, soil pH is a key environmental control over NH_3 production in soils (Dawson, 1977; Nelson, 1982). Since NH_3 is typically produced through the deprotonation of NH_4^+, NH_3 emissions would be expected to be higher in relatively alkaline soils, or in soil with alkaline microsites. Globally, soils tend to shift from alkaline to acidic when mean annual precipitation exceeds mean annual evapotranspiration (Slessarev et al., 2016), so soils in drier biomes such as deserts and grasslands tend to be alkaline (though there are exceptions to this pattern), creating conditions favourable to NH_3 volatilization. For example, the combination of pH and ammonium concentrations in soils from a semi-arid ecosystem in Senegal have been shown to create conditions favorable to the emission of NH_3 (Delon et al., 2017).

15   Given the importance of rainfall seasonality, soil pH, and N availability in contributing to NH_3 emission pulses, soils in the Sahel may be an important source of NH_3 to the atmosphere during the onset of the rainy season. As such, the Sahel is a good region to focus on in determining whether Birch effect NH_3 pulsing is an important process at broad regional scales. The Sahel is a grassland environment representing a transition between desert and productive savannas. It is characterized by a unimodal rainfall seasonality, with mean annual precipitation typically ranging between 100 and 600 mm yr^{-1}. Seasonal variation in rainfall is broadly determined by movement of the Intertropical Convergence Zone (ITCZ). Migration of the ITCZ north of the equator in the first half of the calendar year is accompanied by the onset of the rainy season and West African Monsoon, with the first substantial rain events occurring in April. The southward retreat of the ITCZ marks the dry season starting in October or November. The onset of the rainy season is accompanied by rapid mineralization of nitrogen following the wetting of dry soils in East Africa (Semb and Robinson, 1969), and soil NH_3 emission have been shown to be higher at a site in northern Senegal following a rain event (Delon et al., 2017). Recent maps of African soils based on surface reflectance suggest that soils across the Sahel

tend to have pHs largely near neutral, but can be higher than 9 in some areas (Vågen et al., 2016). The combination of seasonal rainfall variability and soils with neutral or alkaline pHs suggests that Sahelian soils may be an important source of NH$_3$ at the onset of the rainy season. Although the Sahel has regions of relatively dense cropland, it is characterized by lower levels of fertilizer inputs (FAO,

5   accessed 2018) and smaller loads of atmospheric N deposition (Dentener et al., 2006; Galy-Lacaux and Delon, 2014; Laouali et al., 2012), though deposition can be elevated at the Sahel's southern boundary) than other parts of the world. However, it has moderately high livestock densities (Robinson et al., 2014), potentially providing sites of abundant available N for the production of NH$_3$.

10   Earlier work using total column observations from the GOME instrument presented evidence of high atmospheric concentrations of nitrogen dioxide (NO$_2$) over the Sahel in the early rainy season of 2000, which appeared to broadly correspond to rainfall events in the region (Jaeglé et al., 2004). These early growing season increases in tropospheric NO$_2$ concentrations could not be attributed to lightning or to biomass burning, leaving soil emissions the presumed source. Soils emit NO through a variety of

15   biotic and abiotic mechanisms; in the atmosphere, NO rapidly interconverts to NO$_2$, and the two gases are collectively referred to as NO$_x$. Inverse modeling subsequently suggested that soil emissions of NO across sub-Saharan Africa were of the same magnitude as emissions from biomass burning, which previously had been thought to be the dominant NO$_x$ source in the region.

20   At regional scales, the processes controlling intra-annual variability in emissions, and the magnitude of emission responses to these controls, are not well constrained. Atmospheric models often rely on static emissions inventories of NH$_3$ that lack intra-annual variability or detailed environmental controls over emissions from soils (e.g., Bouwman et al., 1997; European Commission, Jount Research Center (JRC)/Netherlands Environmental Agency (PBL), 2011; Lamarque et al., 2010), particularly for

25   natural ecosystems (e.g., Paulot and Jacob, 2014). Fire emission inventories are generally created using data on burned area, fuel load, combustion completeness, and emission factors that translate total carbon or dry matter emissions into trace gas or aerosol emissions into account, producing daily emissions estimates at 0.25° resolution (e.g., van der Werf et al., 2017). Inventories of NH$_3$ emissions from

natural soils tend to rely on a global estimate for the year 1990 (Bouwman et al., 1997) and agricultural emission inventories with sub-annual temporal resolution tend not to consider environmental controls other than temperature and wind speed (e.g., Paulot and Jacob, 2014).

5   Here we use satellite retrievals of atmospheric NH_3 concentrations (Whitburn et al., 2016) over Africa to evaluate whether the onset of the rainy season causes pulsed emissions of NH_3 over the Sahel, focusing on the year 2008, and evaluate its environmental drivers. We compare the seasonal pattern in atmospheric NH_3 concentrations observed by satellite to monthly surface NH_3 deposition measured at 7 sites in north equatorial Africa. We also use a simple box model to calculate surface fluxes based on

10   retrieved atmospheric concentrations, and compare modeled surface fluxes to NH_3 emissions from biomass burning as quantified in the Global Fire Emissions Database 4s (GFED4s; van der Werf et al., 2017). Finally, we also make comparisons to modeled surface fluxes of NO_x derived from NO_2 observations made by the Ozone Monitoring Instrument (OMI; Krotkov, accessed 2018).

2. Methods

15   **2.1 Satellite products**

The Infrared Atmospheric Sounding Interferometer (IASI-A), launched aboard the European Space Agency's MetOp-A in 2006, obtains retrievals of atmospheric NH_3 at a global distribution and bi-daily resolution. IASI-A is a polar-orbiting instrument in a sun-synchronous orbit (9:30 Local Solar Time equator crossing, descending node), providing two observations daily; here we use morning

20   observations, when the thermal contrast is more favorable for retrievals (Clarisse et al., 2009; Van Damme et al., 2014). IASI-A provides a horizontal resolution of 12 km over a swath width of about 2,200 km. The retrieval product used follows the approach implemented by Whitburn *et al.* (2016), in which total columns of NH_3 are obtained by calculating a dimensionless spectral index (HRI), which is then converted into a NH_3 total column through the use of a neural network. The neural network uses a

25   range of variables such as temperature and water vapor profiles to represent the state of the atmosphere as best as possible to produce the matching NH_3 total column for that atmospheric state. Retrievals with

errors above 100% were excluded from the analysis, though exceptions were made for low concentrations, which tend to have a higher error, when the following condition was met:

$$\text{Retrieval error} \times \text{total column NH}_3 \times 0.01 < 5 \times 10^{15} \qquad (1)$$

where the retrieval error is a percentage and the total column NH_3 is a concentration in molecules cm^{-2}. In addition, only retrievals that were at least 75% cloud-free were used. We regridded the Level-2 IASI NH_3 product to $0.25° \times 0.25°$ resolution to match the resolution of soil moisture and other data used in the analysis. The IASI product has been validated using ground-based Fourier transform infrared (FTIR) observations of NH_3 total columns, with robust correlations at sites with high NH_3 concentrations, but lower at sites where atmospheric concentrations approach IASI's detection limits (Dammers et al., 2017). Compared to the FTIR observations the IASI total columns are biased low by ~30% which varies per region depending on the local concentrations.

15   We used the Tropical Rainfall Measuring Mission (TRMM) daily precipitation product (3B42), which is based on a combination of TRMM observations, geo-synchronous infrared observations, and rain gauge observations (Huffman et al., 2007). Independent rain gauge observations from West Africa have been used to validate the product, with no indication of bias in the product (Nicholson et al., 2003).

20   We used the European Space Agency's Climate Change Initiative (ESA-CCI) 30-year daily soil moisture product gridded at $0.25° \times 0.25°$ resolution (Dorigo et al., 2017; Gruber et al., 2017; Liu et al., 2012). The product is based on both passive and active microwave sensors, and has been validated globally (Dorigo et al., 2014) and in East Africa (McNally et al., 2016). Although the product exhibited moderate correlation with ground observations globally, it provides relatively high correlations (r~0.7) for West African sites when seasonality is included in the analysis (Dorigo et al., 2014).

We also used the publicly available level 3 tropospheric NO_2 concentrations product from OMI, a nadir-viewing spectrometer measuring solar backscatter in the UV-visible range aboard NASA's Aura satellite (Krotkov et al., 2017). The product is cloud-screened, including only pixels with less than 30% cloud cover, and presented in at 0.25° × 0.25° resolution. The OMI product relies on air mass factors

5   calculated with the assistance of an atmospheric chemical transport model, and is sensitive to model representations of emission, chemistry and transport data. These are generally poorly constrained for regions not commonly analyzed in chemical transport models such as sub-Saharan Africa (McLinden et al., 2014). Additional bias may be introduced due to the reliance on nearly cloud-free pixels, where greater sunlight may induce higher photochemical rates. For example, the current product is biased

10   roughly 30% low over the Canandian oil sands (McLinden et al., 2014). Level 2 OMI-NO_2 product has been validated against in situ and surface-based observations showing good agreement (Lamsal et al., 2014). In statistical analyses, soil moisture, precipitation, and NO_2 data were masked to match pixels for which NH_3 retrievals were also available.

2.2 Surface flux calculations

15   A range of possible surface fluxes of NH_3 and NO_2 from our focal study region in the Sahel, ranging from 10° to 16°N and from 0°E to 30°E, were calculated from IASI total column NH_3 concentrations and OMI-NO_2 tropospheric concentrations using a simple box model (Jacob, 1999). The specific region was selected as representative of the Sahel, and to allow for direct comparisons to earlier work examining NO_2 emissions from the region (Jaeglé et al., 2004). Daily mean gridded

20   concentrations of retrievals for each gas were averaged across the focal region with units of molecules cm^{-2}. The mean total column concentrations of gas x were converted to a mean surface density for the region in units of kg m^{-2} for each day, using the following equation:

$$M_{x,t} = (TC_{x,t} \times MM_x \times 10)/N_a \qquad (2)$$

where $M_{x,t}$ is the mean surface density of gas x for day t, $TC_{x,t}$ is the average of retrieved total columns of gas x in units of molecules cm^{-2} for day t, MM_x is the molar mass of gas x, and N_a is Avogadro's

number. The dividend on the right hand of the equation is multiplied by 10 to convert the mean surface density to units of kg m^{-2}. This mean surface density was then used in the box model to calculate a mean surface flux for each day, assuming first order losses of gas x:

5    $E_{x,t}(mol) = (M_{x,t} - M_{x,t-d}e^{-d/\tau x})/(\tau_x (1 - e^{-d/\tau x})$ (3)

where $E_{x,t}$ is the surface flux on day t in units of kg m^{-2} day^{-1}, d is the time between subsequent observations (one day in this study), and τ_x is the effective lifetime of a molecule of gas x, including both reactive and transport losses. As both the effective lifetime and the surface flux are unknowns in

10   the equation, we use a range of plausible lifetimes for each gas to calculate a range of surface fluxes. For NH$_3$, we use lifetimes of 6, 12, 24, and 36 hours (Dentener and Crutzen, 1994; Whitburn et al., 2015); for NO$_2$, we use lifetimes of 6, 12, and 24 hours (Beirle et al., 2011; de Foy et al., 2015; Jena et al., 2014). The values were selected to reflect the possible range of lifetimes throughout the year, including periods of elevated wet deposition during the rainy season.

15   **2.3 Emissions inventory**

GFED4s (van der Werf et al., 2017) provides monthly fire emissions at 0.25° resolution based on satellite-derived burned area (Giglio et al., 2013; Randerson et al., 2012) and a modified version of the Carnegie-Ames-Stanford-Approach (CASA) biogeochemical model (Potter et al., 1993). Daily emissions are calculated using data on the fraction of monthly emissions emitted on each date.

20   Uncertainty in GFED fire emissions stems from uncertainty in burned area, fuel consumption, and emission factors but is poorly constrained. According to van der Werf *et al.* (2017) a 1σ of about 50% for fire carbon emissions is reasonable for continental scale estimates. This may also be a best-guess estimate for fire NH3 emissions in our study region; while the uncertainty in NH3 emission factors is large because few fires have been sampled and adds to the total uncertainty, burned area and fuel

25   consumption in savannas is in general better constrained than in other biomes.

2.4 Statistical analyses

Pearson product moment correlation analyses were conducted using pearsonr from the scipy.stats package in Python v3.6.3.

5   **3. Results and Discussion**

The wetting of dry soils has been known to stimulate biogeochemical cycling since at least the 1950s. Its role in creating large pulsed emissions of trace gases such as CO_2 and NO_2 has been demonstrated at laboratory (e.g., Birch and Friend, 1956), field (e.g., Davidson, 1992), and regional scales through satellite observations (Jaeglé et al., 2004) and observation networks (Adon et al., 2010).

10   Evidence for its importance to emissions of NH_3 has been limited to a few laboratory and field studies, with sometimes contrasting results, and its importance at landscape or regional scales is not well constrained. Here we present evidence that the Birch effect is an important driver of NH_3 emissions at regional scales, and likely responsible for the periods of the highest atmospheric NH_3 concentrations over the Sahel region in Africa.

3.1 Seasonal variability in NH_3 concentrations over Africa

Atmospheric NH_3 concentrations in 2008 exhibited broad seasonality that appears to correspond to seasonal precipitation patterns across the continent (Figure 1). In January, mean monthly concentrations are highest across a latitudinal band from roughly 5° N to 10° N, broadly corresponding

20   to the region of highest biomass burning emissions (Figure 1). In April, higher cumulative monthly precipitation across the southern Sahel coincides with increased mean monthly NH_3 concentrations in the focal region (the red box in figure 1b); fire emissions are generally absent across the Sahel and much of the rest of the continent in April, with some emissions occurring along coastal West Africa. By August, during the middle of the West African Monsoon, hotspots of ammonia concentrations are

25   generally absent from the continent, though concentrations are slightly elevated in central southern Africa, where emissions from biomass burning are also elevated (Figure 1).

3.2 Evidence for precipitation-induced emissions of NH$_3$ in the Sahel

For our focal region of the Sahel (defined above and outlined in red in Figure 1), mean atmospheric NH$_3$ concentrations exhibit two distinct peaks in late March and April (Figure 2a, highlighted in light and dark pink, respectively), which represent the highest concentrations observed in 2008. The peak in April, during which atmospheric NH$_3$ concentrations over the Sahel are elevated relative to other parts of north equatorial Africa (Figure 3a), occurs during the first period of sustained rainfall in the focal region, and corresponds to a peak in soil moisture, suggesting a possible causal relationship between changes in soil moisture and atmospheric NH$_3$ concentrations (Figure 2b and section 3.2.1 below). The late March peak occurs at the same time as an apparent modest increase in mean soil moisture (Fig 2b), but also as a possible modest increase mean fire emissions (Fig 2a) across the Sahel. Overall, however, the seasonality in IASI-retrieved atmospheric NH$_3$ concentrations exhibits a marked difference from the seasonality in GFED4s NH$_3$ emissions from fires, which start increasing in September and peak in November (Fig 2a and section 3.2.2 below).

3.2.1 Soil moisture controls over early growing season atmospheric NH$_3$ concentrations

Multiple lines of evidence support a causal relationship between changes in soil moisture and atmospheric NH$_3$ concentrations across the Sahel. Foremost are the significant correlations between ESA-CCI's soil moisture product and the IASI total column during the onset of the rainy season. Specifically, for the period from February 23 to May 1, 2008, there is a significant correlation between mean atmospheric NH$_3$ concentrations of all pixels with acceptable retrievals in the Sahel focal region and mean soil moisture across the same set of pixels (r=0.28, P=0.02; Figure 4a). This correlation integrates all pixels across the Sahel, and thus excludes any sub-regional spatial structure in the data. To examine whether a relationship between soil moisture and NH$_3$ concentrations is also present at a finer spatial scale, we conducted a correlation between the two variables for each pixel for which both variables were present during April, and again found a significant positive linear correlation (r=0.16, p<0.001; Figure 4b). Maps of 3-day averages for precipitation, soil moisture, and total column NH$_3$ concentration over the southern Sahel at 0.25° resolution illustrate the changes in each variable that

occur during the development of the April emissions peak (Figure 5). Between April 13 and April 27, precipitation events in the southern half of the focal region (left-hand column) appear to be accompanied by steady increases in soil moisture (middle column) and total column NH_3 (right-hand column).

Although the explanatory power of the correlations between ESA-CCI's soil moisture product and the IASI total column NH_3 concentrations is relatively low, it demonstrates a broad regional correlation between NH_3 concentrations and changes in soil moisture at the onset of the rainy season – a relationship that is strong enough to be observed at the scale of the Sahel. To provide some context for
10 the statistical result, earlier work finding that rainfall is responsible for large emissions of NO_2 in the same region did not include any statistical analysis in support of its findings (Jaeglé et al., 2004), and studies using satellite observations to infer environmental controls interpret correlation coefficients on the order of 0.25 to be evidence of a strong effect (e.g., Andela et al., 2017).

15 **3.2.2 Minimal contribution of fire emissions to early growing season pulses**

We can further exclude biomass burning as the source of the observed pulses of atmospheric NH_3. Biomass burning occurs in the Sahel with a well-known seasonality as based on several independent satellite fire metrics such as burned area and active fire detections (Duncan, 2003;
20 Giglio et al., 2006). In general, burning in the Sahel occurs in the second half of the year, and few emissions are expected at the onset of the rainy season (Figure 1, 2). A comparison between our box model estimates of NH_3 flux and emissions from the GFED4s inventory strongly supports the hypothesis that biomass burning does not play an important role in NH_3 emissions during March or April, and further suggests that biomass burning may represent a relatively unimportant regional source
25 of NH_3 during most of the year (Figure 6). The modelled total surface flux based on IASI observations varies depending on the effective lifetime used by up to a factor of roughly 4, with seasonal patterns mirroring the patterns in atmospheric concentration, and the largest emissions occurring during the pulses in March and April (Figure 6). In contrast, fire emissions of NH_3 from GFED4s are

concentrated in the second half of the year, and are negligible during March and April, suggesting that they do not contribute to the early growing-season emission pulses.

The importance of a source of NH_3 other than biomass burning in equatorial North Africa was suggested earlier for 0 to 10° N, a region immediately south of the Sahel and of the southern boundary of our focal region in Figures 1 and 2 (Van Damme et al., 2015; Whitburn et al., 2015). Whitburn *et al.* observe a one to two-month lag between peak fire radiative power and IASI- NH_3 that differs from the pattern of IASI carbon monoxide (CO) concentrations, suggesting that fire emissions can explain only some of the atmospheric NH_3 present. They speculate that soils may be the source of NH_3 emissions following the fire season, perhaps resulting from an increase in volatilization caused by increasing soil temperatures and pH, though the paper is focused on evaluating fire emissions and they do not test this hypothesis (Whitburn et al., 2015). Van Damme *et al.* speculate that the emissions are agricultural in nature (Van Damme et al., 2015). IASI-NH_3 concentrations in the other regions examined (southern Africa, Southeast Asia, and central South America) generally track fire activity, or are thought to be due to anthropogenic emissions (Whitburn et al., 2015). Although we have focused on the Sahel, it seems possible that the seasonality of rainfall in environments further south, between 0 and 10° N, could partly explain the elevated emissions observed there following the end of the fire season.

3.2.3 Co-emission of NH_3 and NO_2

The peak in NH_3 concentrations in April occurs at the same time as a peak in NO_2 concentrations (though unlike NH_3, the April peak does not represent the highest annual atmospheric concentration of NO_2). For the entire month of April, total column NH_3 concentrations and tropospheric NO_2 concentrations are strongly correlated (r=0.78, p<0.0001). The simultaneous increase in atmospheric NO_2 and NH_3 concentrations provides additional, indirect support for a soil source of NH_3 (Figure 2, 6). In addition to abundant field- and laboratory evidence that previously dry soils emit large pulses of NO following wetting (Davidson, 1992; Davidson et al., 1991; Dick et al., 2001; Meixner et al., 1997), Jaegle *et al.* (2004) showed that this soil NO pulse is responsible for the highest

concentrations of atmospheric NO_2 over the same region we focused on. As with the seasonal pattern in NH_3 concentrations, seasonal variation in OMI-NO_2 tropospheric concentrations does not match that of the GFED4s NO_2 emissions from fires (Figure 6). We believe that the simplest explanation for our box model results showing the strong correlation between tropospheric NO_2 and total column NH_3

5 concentrations in April is that the two pulses are the result of soil emissions triggered by the same environmental change—in this case, an increase in soil moisture following an extended dry period.

Like NH_3, concentrations of NO_2 also exhibit a peak in mid-March, but the peak lags a week behind the NH_3 peak (Figure 2). Although NO emissions from soils can peak within hours after wetting

10 (Davidson, 1992), in a laboratory setting using soils from the Mojave Desert, an NO pulse lagged 1 to 2 days behind an NH_3 pulse following experimental wetting (McCalley and Sparks, 2008). The authors argue that this lag may be related to competition for NH_4^+ between NH_3 volatilization and nitrification, with volatilization generally outcompeting nitrification during the initial period following wetting. An alternative or additional contributing factor to the lag may be related to the population dynamics of

15 nitrifying bacteria. Although the transcriptional response of nitrifiers to wetting can be very rapid (Placella and Firestone, 2013), at a population level nitrifiers are generally slow-growing (Robertson and Groffman, 2007), suggesting that populations in resource-limited environments may not be able to immediately take advantage of sudden large increases in resource availability. For example, NO emission responses to inorganic N inputs—which arguably provides a similar immediate release from a

20 resource limitation as wetting of dry soils for nitrifiers, particularly in relation to the presumed increase in NH_4^+ concentrations caused by wetting—exhibited pulse responses that lagged roughly a week behind fertilizer additions in Kenya (Hickman et al., 2017). In the case of the Sahel, nitrifier populations may not be able to recover quickly from the extended dry conditions in March, and the lagged emission response of NO could be explained by the slow population-level response to the flush

25 of mineralized N that follows wetting.

The March NO pulse is also smaller than the April NO pulse, and smaller than the April NH_3 pulse. Field studies have observed larger pulses following the second rainfall of the season (Meixner et

al., 1997). The initial increase in soil moisture during March was modest (Figure 2), so it seems possible that soils dried out quickly, before populations of nitrifying bacteria grew large enough to trigger an NO pulse of the magnitude that occurs in April. Increased competition for available NH_4^+ by nitrifying bacteria in April may have limited the NH_3 pulse.

Although earlier researchers have hypothesized that NH_3 volatilization and nitrification cannot co-occur in the same soils (Praveen-Kumar and Aggarwal, 1998), the few field and lab studies measuring soil emissions of both gases following wetting observe positive fluxes of each (McCalley and Sparks, 2008; Schlesinger and Peterjohn, 1991; Soper et al., 2016), with NH_3 dominating emissions
10   from desert soils (McCalley and Sparks, 2008; Schlesinger and Peterjohn, 1991) and NO_2 dominating from grassland soils (Soper et al., 2016). We expect that even were the two processes mutually exclusive at the scale of a soil core or chamber, heterogeneity in soil properties at the pixel or regional scale can explain our observations of coinciding pulses of NO and NH_3.

15   **3.3 Magnitude and importance of soil NH_3 emission pulses**

During the early growing season, atmospheric concentrations of NH_3 are roughly an order of magnitude higher than NO_2 (figure 2). It is important to note that NH_3 retrievals generally have a higher error, and that our screening process may introduce a potential bias in that we permit retrievals with
20   higher uncertainty if they are low concentrations; we also retain observations of negative concentrations. From this perspective, our concentration and emission estimates can be considered conservative.

Because the magnitude of mean surface fluxes depends on the effective lifetime used in the box
25   model, comparisons between the modeled fluxes of NO_2 and NH_3 are not straightforward. In general, however, our modelled emissions suggest that NH_3 is probably emitted at substantially higher rates than NO during pulse events, possibly by a factor of ten or more (figure 6). This result is unexpected, given earlier observations that NH_3 tends to be the dominant source in highly alkaline desert soils (pH 9-11;

McCalley and Sparks, 2008), whereas emissions from grassland soils with a more neutral pH, as might be expected in the Sahel, were dominated by NO, by roughly a factor of 10:1 (Soper et al., 2016). This pulse produces NH_3 concentrations comparable in magnitude to the peak concentrations over many of the Earth's major biomass burning regions (Whitburn et al., 2015). Indeed, NH_3 emissions during the

5 date range February 29-March 16 and April 12-May 1, which cover the two emission peaks during that period, represented about one fifth of annual NH_3 emissions from our focal region in the Sahel (annual emissions of ~0.4 to 2 Tg N, and total pulse emissions of ~0.1 to 0.5 Tg N, depending on the effective lifetime assumed). It is important to note that in addition to uncertainty associated with the NH_3 retrievals, additional sources of bias and uncertainty—such as the use of an effective lifetime rather than

10 explicitly accounting for deposition fluxes and chemistry, uncertainty in the value and variability in that lifetime, and biases in both the IASI and OMI retrievals—limit our ability to quantitatively constrain the surface NH_3 or NO fluxes, or to make strict quantitative comparisons between them.

This substantial pulse of NH_3, and the co-occurrence of a pulse of NO_x, could be an important

15 source of $PM_{2.5}$ in the region during the first half of the year. Secondary inorganic aerosols such as ammonium sulfate are formed in reactions involving NH_3, and ammonium nitrate aerosol formation requires both gaseous NH_3 and NO_x. In the Sahel, combustion sources of NO_x are relatively small in March and April (Fig. 6), making soil NO emissions potentially more important in the formation of $PM_{2.5}$.

20 **3.4 Comparison to surface observations**

The INDAAF network (International Network to Study Deposition and Atmospheric Chemistry in Africa, http://www.indaaf.obs-mip.fr) provides monthly surface NH_3 deposition rates between 1998 to 2016 for seven sites in north equatorial Africa, both in and outside the Sahel. The work of Adon *et al.* (2010) presents an analysis of annual and seasonal variability of surface gases concentrations (NO_2,

25 HNO_3, O_3, SO_2, and NH_3) from the long-term monitoring INDAAF stations over the period 2000-2007. The two sites in the Sahel (Figure 3c (Banizoumbou, Niger) and 3f (Katibougou, Mali)) exhibit broadly similar seasonal patterns, with NH_3 concentration increases starting in April (or March in the 2008 case

of Katibougou, Mali (Figure 3f)), but this seasonal pattern is generally absent in sites outside the Sahel (Figure 3b, 3d, 3e, 3g, and 3h). These seasonal patterns are broadly consistent with the pulsing dynamics observed by IASI in the Sahel, and the absence of pulsing outside the Sahel (Figure 3).

5   An evaluation of seasonal patterns in the network found that emission patterns differ between wet savannah and dry savannah: dry season emissions tend to be higher in wet savannah, where biomass burning dominates annual emissions (Adon et al., 2010). In dry savannah ecosystems, emissions are higher during the wet season, and are likely enhanced by the volatilization of N inputs from agro-pastoralism in the region, leading to high total N deposition fluxes (Adon et al., 2010). It is conceivable

10 that regional differences in soil pH (Vågen et al., 2016) could also result in different rates of soil NH_3 emissions. In addition, higher leaf area index in wet savannahs and forest could result in more interception of NH_3, reducing soil contributions to atmospheric concentrations during the wet season.

3.5 Later growing season NH_3 emissions

      After the early season pulses, NH_3 concentrations and fluxes remain fairly elevated (figure 2, 6); during this period, NO_2 concentrations and fluxes increase, becoming comparable in magnitude to NH_3 (figure 2,6). This pattern is consistent with earlier studies describing elevated concentrations of these gases in or near our focal study region for several months following the end of the biomass burning

20 season (Jaeglé et al., 2004; Whitburn et al., 2015). Jaegle *et al.* attribute these elevated concentrations to the wetting of dry soils, and Whitburn et al to the possible acidification of soils. An additional explanation is that these emissions may be associated with agricultural activity. The mean start of the cropping season ranges from May to August in the focal region, based on NDVI-based observations of plant phenology (Vrieling et al., 2011), suggesting that the bulk of elevated NO_2 and NH_3 emissions in

25 the region occur after planting, and well into the rainy season. Elevated emissions could be associated with soil disturbance from tillage (e.g., Yang et al., 2015) or from the use of fertilizer inputs, which have been argued to be higher than generally acknowledged in the scientific and development literature

(Cobo et al., 2010; Sheahan and Barrett, 2017), though N additions in Sahelian countries such as Niger tend to be very low, even for farmers who use fertilizer (Masso et al., 2017; Sheahan and Barrett, 2017).

3.6 Possible sources of error and bias

5   It is worth noting that the morning overpass time used in this analysis is likely to cause a further underestimation of daily NH_3 concentrations, as emissions would be expected to follow diurnal temperature variation and be higher in the afternoon (Van Damme et al., 2015). A more sophisticated inverse modelling approach could provide firmer insight into the magnitude of emissions, as well as provide some insight into the magnitude of specific NH_3 sources. Our analysis is subject to several

10   additional sources of uncertainty: increased cloud cover during the rainy season tends to result in fewer observations than during the dry season, so our regional means are based on different numbers of observations at different times of year.

    Although the explanatory power of the linear relationship between soil moisture and emissions

15   in the early part of the rainy season is relatively low, this would be expected in part as we would expect the relationship to be complex and to vary over time. Multiple studies have shown that rewetting of dry soils results in lower emission pulses for the same level of water addition (Davidson, 1992; Davidson et al., 1991), including of NH_3 emissions (Soper et al., 2016). It also seems plausible that there are threshold effects in which an initial increase in soil moisture may simply need to be large enough to

20   activate dormant microbial communities and/or cause a flush of labile microbial N to trigger an emissions pulse, such that the pulse response might best be described with a piecewise function. Asynchrony between plant and microbial activity during soil wet up and dry down (Collins et al., 2008), and different activation thresholds for microbial and plant responses to precipitation (Dijkstra et al., 2012) may also play a role in determining the amount of available NH_4^+ for volatilization at different

25   times in the early rainy season.

3.7 Conclusion

Satellite measurements of trace gases—although not without their limitations—provide a powerful tool for understanding global and regional atmospheric composition, and for gaining insights into the controls over nitrogen cycling and trace gas emissions, particularly for regions where other types of measurements are scarce. With daily observed and observation-based data available for

5 multiple environmental variables including precipitation, soil moisture, biomass burning emissions, and tropospheric NO_2 concentrations, it is possible to evaluate specific mechanisms behind the seasonality of trace gas emissions. In an evaluation of the Sahel during 2008, we find that NH_3 concentrations are elevated during March and April, a period when biomass burning emissions are absent, but when tropospheric NO_2 concentrations exhibit similar temporal dynamics. We further find that the increase in

10 NH_3 concentrations are positively correlated to changes in soil moisture at the start of the rainy season. Using a simple box model, we estimate that average emissions for the entire Sahel are between 2 and 6 mg NH_3 m^{-2} day^{-1} during peaks of the observed pulses, though note that these estimates are subject to substantial bias and uncertainty. We conclude that the Birch effect is an important and geographically broad driver of NH_3 emissions, and am important component of the N cycle in the Sahel.

References

Adon, M., Galy-Lacaux, C., Yoboue, V., Delon, C., Lacaux, J. P., Castera, P., Gardrat, E., Pienaar, J., Ourabi, Al, H., Laouali, D., Diop, B., Sigha-Nkamdjou, L., Akpo, A., Tathy, J. P., Lavenu, F. and Mougin, E.: Long term measurements of sulfur dioxide, nitrogen dioxide, ammonia, nitric acid and

20 ozone in Africa using passive samplers, Atmos. Chem. Phys., 10, 7467–7487, doi:10.5194/acp-10-7467-2010, 2010.

Andela, N., Morton, D. C., Giglio, L., Chen, Y., van der Werf, G. R., Kasibhatla, P. S., DeFries, R. S., Collatz, G. J., Hantson, S., Kloster, S., Bachelet, D., Forrest, M., Lasslop, G., Li, F., Mangeon, S., Melton, J. R., Yue, C. and Randerson, J. T.: A human-driven decline in global burned area, Science,

25 356, 1356–1362, doi:10.1126/science.aal4108, 2017.

Anderson, I. C. and Levine, J. S.: Relative rates of nitric oxide and nitrous oxide production by nitrifiers, denitrifiers, and nitrate respirers, Applied and Environmental Microbiology, 51(5), 938–945, 1986.

Austin, A. T., Yahdjian, L., Stark, J. M., Belnap, J., Porporato, A., Norton, U., Ravetta, D. A. and Schaeffer, S. M.: Water pulses and biogeochemical cycles in arid and semiarid ecosystems, Oecol., 141(2), 221–235, doi:10.1007/BF00335913, 2004.

5   Beirle, S., Boersma, K. F., Platt, U., Lawrence, M. G. and Wagner, T.: Megacity emissions and lifetimes of nitrogen oxides probed from space, Science, 333(6050), 1737–1739, doi:10.1126/science.1207824, 2011.

Bergstrom, A.-K. and Jannson, M.: Atmospheric nitrogen deposition has caused nitrogen enrichment and eutrophication of lakes in the northern hemisphere, Global Change Biol., 12, 635–643, doi:10.1111/j.1365-2486.2006.01129.x, 2006.

10   Birch, H. F.: The effect of soil drying on humus decomposition and nitrogen availability, Plant Soil, 10, 9–31, 1958.

Birch, H. F.: Nitrification in soils after different periods of dryness, Plant Soil, 12, 81–96, 1960.

Birch, H. F. and Friend, M. T.: Humus decomposition in East African soils, Nature, 178, 500–501, 1956.

15   Bobbink, R., Hicks, K., Galloway, J., Spranger, T., Alkemade, R., Ashmore, M., Bustamante, M., Cinderby, S., Davidson, E. and Dentener, F.: Global assessment of nitrogen deposition effects on terrestrial plant diversity: a synthesis, Ecol. Appl., 20, 30–59, 2010.

Borken, W. and Matzner, E.: Reappraisal of drying and wetting effects on C and N mineralization and fluxes in soils, Global Change Biol., 15, 808–824, doi:10.1111/j.1365-2486.2008.01681.x, 2009.

20   Bouwman, A. F., Lee, D. S. and Asman, W.: A global high-resolution emission inventory for ammonia, Global Biogeochem. Cy., 11, 561–587, 1997.

Clarisse, L., Clerbaux, C., Dentener, F., Hurtmans, D. and Coheur, P.-F.: Global ammonia distribution derived from infrared satellite observations, Natur Geosci., 2, 479–483, doi:10.1038/ngeo551, 2009.

Cobo, J. G., Dercon, G. and Cadisch, G.: Nutrient balances in African land use systems across different 25   spatial scales: A review of approaches, challenges and progress, Agric., Ecosys. Environ., 136, 1–15, doi:10.1016/j.agee.2009.11.006, 2010.

Collins, S. L., Sinsabaugh, R. L., Crenshaw, C., Green, L., Porras-Alfaro, A., Stursova, M. and Zeglin, L. H.: Pulse dynamics and microbial processes in aridland ecosystems, J. Ecol., 96, 413–420, doi:10.1111/j.1365-2745.2008.01362.x, 2008.

30   Dammers, E., Shephard, M. W., Palm, M., Cady-Pereira, K., Capps, S., Lutsch, E., Strong, K., Hannigan, J. W., Ortega, I., Toon, G. C., Stremme, W., Grutter, M., Jones, N., Smale, D., Siemons, J.,

Hrpcek, K., Tremblay, D., Schaap, M., Notholt, J. and Erisman, J. W.: Validation of the CrIS Fast Physical NH₃ Retrieval with ground-based FTIR, Atmos. Meas. Tech. Discuss., 10, 2645-2667, doi:10.5194/amt-2017-38-AC2, 2017.

5   Davidson, E. A.: Pulses of nitric oxide and nitrous oxide flux following wetting of dry soil: An assessment of probable sources and importance relative to annual fluxes, Ecol. Bull., 149–155, 1992.

Davidson, E. A., Vitousek, P. M., Matson, P. A., Riley, R., García-Méndez, G. and Maass, J. M.: Soil emissions of nitric oxide in a seasonally dry tropical forest of México, J. Geophys. Res.- Biogeosci., 96, 15439–15445, doi:10.1029/91JD01476, 1991.

10 Dawson, G. A.: Atmospheric ammonia from undisturbed land, J. Geophys. Res.-Biogeosci., 82, 3125–3133, 1977.

de Foy, B., Lu, Z., Streets, D. G., Lamsal, L. N. and Duncan, B. N.: Estimates of power plant NOx emissions and lifetimes from OMI NO2 satellite retrievals, Atmos. Environ., 116, 1–11, doi:10.1016/j.atmosenv.2015.05.056, 2015.

15 Delon, C., Galy-Lacaux, C., Serca, D., Loubet, B., Camara, N., Gardrat, E., Saneh, I., Fensholt, R., Tagesson, T., Le Dantec, V., Sambou, B., Diop, C. and Mougin, E.: Soil and vegetation-atmosphere exchange of NO, NH3, and N2O from field measurements in a semi arid grazed ecosystem in Senegal, Atmos. Environ., 156, 36–51, doi:10.1016/j.atmosenv.2017.02.024, 2017.

Dentener, F. J. and Crutzen, P. J.: A three-dimensional model of the global ammonia cycle, Journal of
20 Atmos. Chem., 19, 331–369, doi:10.1007/BF00694492, 1994.

Dentener, F., Drevet, J., Lamarque, J. F., Bey, I., Eickhout, B., Fiore, A. M., Hauglustaine, D., Horowitz, L. W., Krol, M., Kulshrestha, U. C., Lawrence, M., Galy-Lacaux, C., Rast, S., Shindell, D., Stevenson, D., Van Noije, T., Atherton, C., Bell, N., Bergman, D., Butler, T., Cofala, J., Collins, B., Doherty, R., Ellingsen, K., Galloway, J., Gauss, M., Montanaro, V., Müller, J. F., Pitari, G., Rodriguez,
25 J., Sanderson, M., Solmon, F., Strahan, S., Schultz, M., Sudo, K., Szopa, S. and Wild, O.: Nitrogen and sulfur deposition on regional and global scales: A multimodel evaluation, Glob. Biogeochem. Cy., 20, GB4003, doi:10.1029/2005GB002672, 2006.

Dick, J., Skiba, U. and Wilson, J.: The Effect of Rainfall on NO and N₂O Emissions from Ugandan Agroforest Soils, Phyton, 41, 73–80, 2001.

30 Dijkstra, F. A., Augustine, D. J., Brewer, P. and Fischer, von, J. C.: Nitrogen cycling and water pulses in semiarid grasslands: are microbial and plant processes temporally asynchronous? Oecol., 170, 799–808, doi:10.1007/s10021-010-9341-6, 2012.

Dorigo, W. A., Gruber, A., De Jeu, R. A. M., Wagner, W., Stacke, T., Loew, A., Albergel, C., Brocca, L., Chung, D., Parinussa, R. M. and Kidd, R.: Evaluation of the ESA CCI soil moisture product using ground-based observations, Remote Sens. Environ., 162, 380-395, doi:10.1016/j.rse.2014.07.023, 2014.

5 Dorigo, W., Wagner, W., Albergel, C., Albrecht, F., Balsamo, G., Brocca, L., Chung, D., Ertl, M., Forkel, M., Gruber, A., Haas, E., Hamer, P. D., Hirschi, M., Ikonen, J., de Jeu, R., Kidd, R., Lahoz, W., Liu, Y. Y., Miralles, D., Mistelbauer, T., Nicolai-Shaw, N., Parinussa, R., Pratola, C., Reimer, C., van der Schalie, R., Seneviratne, S. I., Smolander, T. and Lecomte, P.: ESA CCI Soil Moisture for improved Earth system understanding: State-of-the art and future directions, Remote Sens. Environ., 203, 185–
10 215, doi:10.1016/j.rse.2017.07.001, 2017.

Duncan, B. N.: Interannual and seasonal variability of biomass burning emissions constrained by satellite observations, J. Geophys. Res.-Biol., 108, 73–28, doi:10.1029/2002JD002378, 2003.

Eickenscheidt, N., Brumme, R. and Veldkamp, E.: Direct contribution of nitrogen deposition to nitrous oxide emissions in a temperate beech and spruce forest – a ^{15}N tracer study, Biogeosci., 8, 621–635,
15 doi:10.5194/bg-8-621-2011, 2011.

Emmerich, W. E.: Carbon dioxide fluxes in a semiarid environment with high carbonate soils, Agr. Forest Meteorol., 116, 91–102, doi:10.1016/S0168-1923(02)00231-9, 2003.

European Commission, Jount Research Center (JRC)/Netherlands Environmental Agency (PBL): Emission Database for Global Atmospheric Research (EDGAR), release version 4.2, [online] Available
20 from: http://edgar.jrc.ed.europa.eu, 2011.

FAO: FAOSTAT database collections, [online] Available from: http://faostat.fao.org, Accessed January 2018

Galy-Lacaux, C. and Delon, C.: Nitrogen emission and deposition budget in West and Central Africa, Environ. Res. Lett., 9, 125002–14, doi:10.1088/1748-9326/9/12/125002, 2014.

25 Giglio, L., Randerson, J. T. and van der Werf, G. R.: Analysis of daily, monthly, and annual burned area using the fourth-generation global fire emissions database (GFED4), J. Geophys. Res.-Biogeosci., 118, 317–328, doi:10.1002/jgrg.20042, 2013.

Giglio, L., van der Werf, G. R., Randerson, J. T., Collatz, G. J. and Kasibhatla, P.: Global estimation of burned area using MODIS active fire observations, Atmos. Chem. Phys., 6, 957–974, doi:10.5194/acpd-
30 5-11091-2005, 2006.

Gruber, A., Dorigo, W. A., Crow, W. and Wagner, W.: Triple Collocation-Based Merging of Satellite Soil Moisture Retrievals, IEEE Trans. Geosci. Remote Sens., 55, 6780–6792, doi:10.1109/TGRS.2017.2734070, 2017.

Hickman, J. E., Huang, Y., Wu, S., Diru, W., Groffman, P. M., Tully, K. L. and Palm, C. A.: Nonlinear response of nitric oxide fluxes to fertilizer inputs and the impacts of agricultural intensification on tropospheric ozone pollution in Kenya, Glob. Change Biol., 23, 3193-3204, doi:10.1029/95JD00370, 2017.

5   Holland, E., Braswell, B., Sulzman, J. and Lamarque, J.: Nitrogen deposition onto the United States and western Europe: Synthesis of observations and models, Ecol. Appl., 15, 38–57, 2005.

Huffman, G. J., Bolvin, D. T., Nelkin, E. J., Wolff, D. B., Adler, R. F., Gu, G., Hong, Y., Bowman, K. P. and Stocker, E. F.: The TRMM Multi-satellite Precipitation Analysis: Quasi-Global, Multi-Year, Combined-Sensor Precipitation Estimates at Fine Scale, J. Hydrometeorol., 8, 38–55,
10   doi:10.1175/jhm560.1, 2007.

Huxman, T. E., Snyder, K. A., Tissue, D., Leffler, A. J., Ogle, K., Pockman, W. T., Sandquist, D. R., Potts, D. L. and Schwinning, S.: Precipitation pulses and carbon fluxes in semiarid and arid ecosystems, Oecol., 141, 254–268, doi:10.1007/s00442-004-1682-4, 2004.

Jacob, D. J.: Introduction to Atmospheric Chemistry, Princeton University Press, Princeton. 1999.

15   Jaeglé, L., Martin, R. V., Chance, K., Steinberger, L., Kurosu, T. P., Jacob, D. J., Modi, A. I., Yoboue, V., Sigha-Nkamdjou, L. and Galy-Lacaux, C.: Satellite mapping of rain-induced nitric oxide emissions from soils, J. Geophys. Res.-Biogeosci., 109, D21310, 2004.

Jena, C., Ghude, S. D., Blond, N., Beig, G., Chate, D. M., Fadnavis, S. and Van der A, R. J.: Estimation of the lifetime of nitrogen oxides over India using SCIAMACHY observations, Intl. J. Remote Sens.,
20   35, 1244–1252, doi:10.1080/01431161.2013.873146, 2014.

Kieft, T., Soroker, E. and Firestone, M. K.: Microbial biomass response to a rapid increase in water potential when dry soil is wetted, Soil Biol. Biochem., 2, 119–126, 1987.

Kim, D. G., Vargas, R., Bond-Lamberty, B. and Turetsky, M. R.: Effects of soil rewetting and thawing on soil gas fluxes: a review of current literature and suggestions for future research, Biogeosci., 9,
25   2459–2483, doi:10.5194/bg-9-2459-2012, 2012.

Krotkov, N. A.: OMI/Aura NO2 Cloud-Screened Total and Tropospheric Column L3 Global Gridded 0.25 degree x 0.25 degree V3, doi:10.5067/Aura/OMI/DATA3007, Accessed January 2018.

Krotkov, N. A., Lamsal, L. N., Celarier, E. A., Swartz, W. H., Marchenko, S. V., Bucsela, E. J., Chan, K. L., Wenig, M. and Zara, M.: The version 3 OMI NO$_2$; standard product, Atmos. Meas. Tech., 10,
30   3133–3149, doi:10.5194/amt-10-3133-2017, 2017.

Lamarque, J. F., Bond, T. C., Eyring, V., Granier, C., Heil, A., Klimont, Z., Lee, D., Liousse, C., Mieville, A., Owen, B., Schultz, M. G., Shindell, D., Smith, S. J., Stehfest, E., Van Aardenne, J.,

Cooper, O. R., Kainuma, M., Mahowald, N., McConnell, J. R., Naik, V., Riahi, K. and van Vuuren, D. P.: Historical (1850–2000) gridded anthropogenic and biomass burning emissions of reactive gases and aerosols: methodology and application, Atmos. Chem. Phys., 10, 7017–7039, doi:10.5194/acp-10-7017-2010, 2010.

5   Lamsal, L. N., Krotkov, N. A., Celarier, E. A., Swartz, W. H., Pickering, K. E., Bucsela, E. J., Gleason, J. F., Martin, R. V., Philip, S., Irie, H., Cede, A., Herman, J., Weinheimer, A., Szykman, J. J. and Knepp, T. N.: Evaluation of OMI operational standard NO_2 column retrievals using in situ and surface-based NO_2 observations, Atmos. Chem. Phys., 14, 11587–11609, doi:10.5194/acp-14-11587-2014, 2014.

10   Laouali, D., Galy-Lacaux, C., Diop, B., Delon, C., Orange, D., Lacaux, J. P., Akpo, A., Lavenu, F., Gardrat, E. and Castera, P.: Long term monitoring of the chemical composition of precipitation and wet deposition fluxes over three Sahelian savannas, Atmos. Environ., 50, 314–327, doi:10.1016/j.atmosenv.2011.12.004, 2012.

Lelieveld, J., Evans, J. S., Fnais, M., Giannadaki, D. and Pozzer, A.: The contribution of outdoor air
15   pollution sources to premature mortality on a global scale, Nature, 525, 367–371, doi:10.1038/nature15371, 2015.

Liu, Y. Y., Dorigo, W. A., Parinussa, R. M., de Jeu, R. A. M., Wagner, W., McCabe, M. F., Evans, J. P. and van Dijk, A. I. J. M.: Trend-preserving blending of passive and active microwave soil moisture retrievals, Remote Sens. Environ., 123, 280–297, doi:10.1016/j.rse.2012.03.014, 2012.

20   Masso, C., Nziguheba, G., Mutegi, J., Galy-Lacaux, C., Wendt, J., Butterbach-Bahl, K., Wairegi, L. and Datta, A.: Soil fertility management in sub-Saharan Africa, in Sustainable Agriculture Reviews, edited by E. Lichtfouse, Springer International Publishing, Cham. 2017.

McCalley, C. K. and Sparks, J. P.: Controls over nitric oxide and ammonia emissions from Mojave Desert soils, Oecol., 156, 871–881, doi:10.1007/s00442-008-1031-0, 2008.

25   McLinden, C. A., Fioletov, V., Boersma, K. F., Kharol, S. K., Krotkov, N., Lamsal, L., Makar, P. A., Martin, R. V., Veefkind, J. P. and Yang, K.: Improved satellite retrievals of NO_2 and SO_2 over the Canadian oil sands and comparisons with surface measurements, Atmos. Chem. Phys., 14, 3637–3656, doi:10.5194/acp-14-3637-2014, 2014.

McNally, A., Shukla, S., Arsenault, K. R., Wang, S., Peters-Lidard, C. D. and Verdin, J. P.: Int. J. Appl.
30   Earth Obs., 48, 96–109, doi:10.1016/j.jag.2016.01.001, 2016.

Meixner, F. X., Fickinger, T., Marufu, L., Serca, D., Nathaus, F. J., Makina, E., Mukurumbira, L. and Andreae, M. O.: Preliminary results on nitric oxide emission from a southern African savanna ecosystem, Nutr. Cy. Agroecosys., 48., 123–138, 1997.

Nelson, D. W.: Gaseous Losses of Nitrogen Other Than Through Denitrification, in Nitrogen in Agricultural Soils, edited by F. J. Stevenson, pp. 327–363, dl.sciencesocieties.org, Madison. 1982.

Nicholson, S. E., Some, B., McCollum, J., Nelkin, E., Klotter, D., Berte, Y., Diallo, B. M., Gaye, I., Kpabeba, G., Ndiaye, O., Noukpozounkou, J. N., Tanu, M. M., Thiam, A., Toure, A. A. and Traore, A.
5   K.: Validation of TRMM and Other Rainfall Estimates with a High-Density Gauge Dataset for West Africa. Part I: Validation of GPCC Rainfall Product and Pre-TRMM Satellite and Blended Products, J. Appl. Meteorol., 42, 1337–1354, doi:10.1175/1520-0450(2003)042<1337:votaor>2.0.co;2, 2003.

Paulot, F. and Jacob, D. J.: Hidden Cost of U.S. Agricultural Exports: Particulate Matter from Ammonia Emissions, Environ. Sci. Technol., 48, 903–908, doi:10.1021/es4034793, 2014.

10 Pilegaard, K., Skiba, U., Ambus, P., Beier, C., Brüggemann, N., Butterbach-Bahl, K., Dick, J., Dorsey, J., Duyzer, J. and Gallagher, M.: Factors controlling regional differences in forest soil emission of nitrogen oxides (NO and N_2O), Biogeosci., 3, 651–661, 2006.

Placella, S. A. and Firestone, M. K.: Transcriptional Response of Nitrifying Communities to Wetting of Dry Soil, Appl. Environ. Microbiol., 79, 3294–3302, doi:10.1128/AEM.00404-13, 2013.

15 Placella, S. A., Brodie, E. L. and Firestone, M. K.: Rainfall-induced carbon dioxide pulses result from sequential resuscitation of phylogenetically clustered microbial groups, Proc. Nat. Acad. Sci., 109, 10931–10936, 2012.

Potter, C. S., Randerson, J. T., Field, C. B., Matson, P. A., Vitousek, P. M., Mooney, H. A. and Klooster, S. A.: Terrestrial ecosystem production: A process model based on global satellite and surface
20 data, Glob. Biogeochem. Cy., 7, 811–841, doi:10.1029/93GB02725, 1993.

Praveen-Kumar and Aggarwal, R. K.: Interdependence of ammonia volatilization and nitrification in arid soils, Nutr. Cy. Agroecosys., 51, 201–207, doi:10.1023/A:1009720003490, 1998.

Randerson, J. T., Chen, Y., van der Werf, G. R., Rogers, B. M. and Morton, D. C.: Global burned area and biomass burning emissions from small fires, J. Geophys. Res.—Biogeosci., 117, G04012,
25 doi:10.1029/2012JG002128, 2012.

Robertson, G. P. and Groffman, P. M.: Nitrogen transformations, edited by E. A. Paul, pp. 341–364, Soil microbiology, ecology, and biochemistry, 3rd edn. Academic/Elsevier, New York. 2007.

Robinson, T. P., Wint, G. R. W., Conchedda, G., Van Boeckel, T. P., Ercoli, V., Palamara, E., Cinardi, G., D'Aietti, L., Hay, S. I. and Gilbert, M.: Mapping the Global Distribution of Livestock, PLoS ONE,
30 9, e96084, doi:10.1371/journal.pone.0096084, 2014.

S Whitburn, S., . van Damme, M., Clarisse, L., Bauduin, S., Heald, C. L., Hadji-Lazaro, J., Hurtmans, D., Zondio, M.A., Clerbaux, C., Coheur, P.-F.: A flexible and robust neural network IASI-NH3 retrieval algorithm, J. Geophys. Res.—Biogeosci., 121, 6581-6599, doi:10.1002/(ISSN)2169-8996, 2016.

Saetre, P. and Stark, J. M.: Microbial dynamics and carbon and nitrogen cycling following re-wetting of
5   soils beneath two semi-arid plant species, Oecol., 142, 247–260, doi:10.1007/s00442-004-1718-9, 2004.

Schlesinger, W. H. and Peterjohn, W. T.: Processes controlling ammonia volatilization from Chihuahuan desert soils, Soil Biol. Biochem., 23, 637–642, 1991.

Semb, G. and Robinson, J. B. D.: The natural nitrogen flush in different arable soils and climates in East Africa, E. Afr. Agric. Forestry J., 34, 350–370, 1969.

10 Sheahan, M. and Barrett, C. B.: Ten striking facts about agricultural input use in Sub-Saharan Africa, Food Policy, 67, 12–25, doi:10.1016/j.foodpol.2016.09.010, 2017.

Slessarev, E. W., Lin, Y., Bingham, N. L., Johnson, J. E., Dai, Y., Schimel, J. P. and Chadwick, O. A.: Water balance creates a threshold in soil pH at the global scale, Nature, 540, 567–569, doi:10.1038/nature20139, 2016.

15 Soper, F. M., Boutton, T. W., Groffman, P. M. and Sparks, J. P.: Nitrogen trace gas fluxes from a semiarid subtropical savanna under woody legume encroachment, Glob. Biogeochem. Cy., 30, 614–628, doi:10.1002/2015gb005298, 2016.

Thomas, R. Q., Canham, C. D., Weathers, K. C. and Goodale, C. L.: Increased tree carbon storage in response to nitrogen deposition in the US, Nature Geosci., 3, 13–17, doi:10.1038/ngeo721, 2009.

20 Tian, D. and Niu, S.: A global analysis of soil acidification caused by nitrogen addition, Environ. Res. Lett., 10, 024019–11, doi:10.1088/1748-9326/10/2/024019, 2015.

Van Damme, M., Clarisse, L., Heald, C. L., Hurtmans, D., Ngadi, Y., Clerbaux, C., Dolman, A. J., Erisman, J. W. and Coheur, P. F.: Global distributions, time series and error characterization of atmospheric ammonia, Atmos. Chem. Phys., 14, 2905–2922, doi:10.5194/acp-14-2905-2014, 2014.

25 Van Damme, M., Erisman, J. W. and Clarisse, L.: Worldwide spatiotemporal atmospheric ammonia (NH3) columns variability revealed by satellite, Geophys. Res. Lett., 42, 8660–8668, doi:10.1002/(ISSN)1944-8007, 2015.

van der Werf, G. R., Randerson, J. T., Giglio, L., van Leeuwen, T. T., Chen, Y., Rogers, B. M., Mu, M., van Marle, M. J. E., Morton, D. C., Collatz, G. J., Yokelson, R. J. and Kasibhatla, P. S.: Global fire
30 emissions estimates during 1997–2016, Earth Syst. Sci. Data, 9, 697–720, doi:10.5194/essd-9-697-2017, 2017.

Vågen, T.-G., Winowiecki, L. A., Tondoh, J. E., Desta, L. T. and Gumbricht, T.: Mapping of soil properties and land degradation risk in Africa using MODIS reflectance, Geoderma, 263, 216–225, doi:10.1016/j.geoderma.2015.06.023, 2016.

Vrieling, A., de Beurs, K. M. and Brown, M. E.: Variability of African farming systems from
5 phenological analysis of NDVI time series, Clim. Change, 109, 455–477, doi:10.1029/2004JD005263, 2011.

Whitburn, S., Van Damme, M. and Clarisse, L.: A flexible and robust neural network IASI-NH3 retrieval algorithm, J. Geophys. Res.-Atmos., 121, 6581–6599, doi:10.1002/(ISSN)2169-8996, 2016.

Whitburn, S., Van Damme, M., Kaiser, J. W., van der Werf, G. R., Turquety, S., Hurtmans, D.,
10 Clarisse, L., Clerbaux, C. and Coheur, P. F.: Ammonia emissions in tropical biomass burning regions: Comparison between satellite-derived emissions and bottom-up fire inventories, Atmos. Environ., 121, 42–54, doi:10.1016/j.atmosenv.2015.03.015, 2015.

Yahdjian, L. and Sala, O. E.: Size of Precipitation Pulses Controls Nitrogen Transformation and Losses
15 in an Arid Patagonian Ecosystem, Ecosystems, 13, 575–585, doi:10.1007/s10021-010-9341-6, 2010.

Yang, Y., Zhou, C., Li, N., Han, K., Meng, Y., Tian, X. and Wang, L.: Effects of conservation tillage practices on ammonia emissions from Loess Plateau rain-fed winter wheat fields, Atmos. Environ., 104, 59–68, doi:10.1016/j.atmosenv.2015.01.007, 2015.
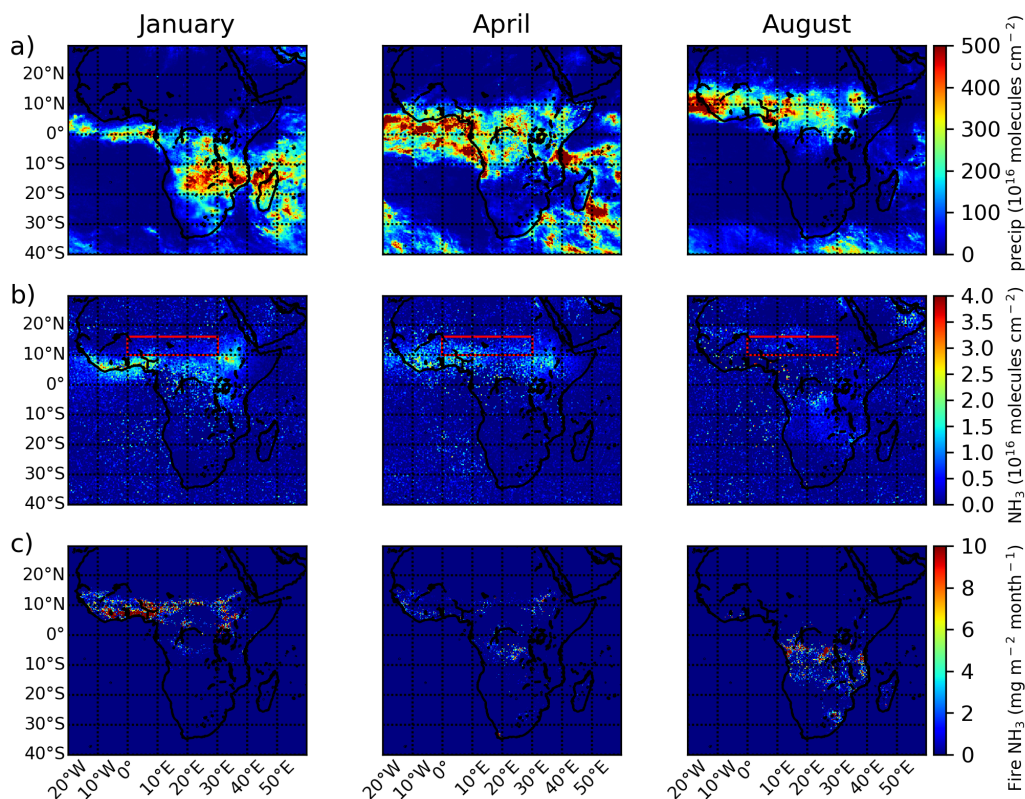
Figure 1. *Seasonality of precipitation and NH₃ emissions in Africa during 2008.* Monthly TRMM precipitation (a), IASI-NH₃ concentrations (b), and GFED4s NH₃ emissions (c) over Africa in January, April, and August, 2008. TRMM precipitation is presented in mm month⁻¹, IASI-NH₃ concentrations in 10¹⁶ molecules cm⁻², and GFED4s NH₃ emissions in mg m⁻² month⁻¹.
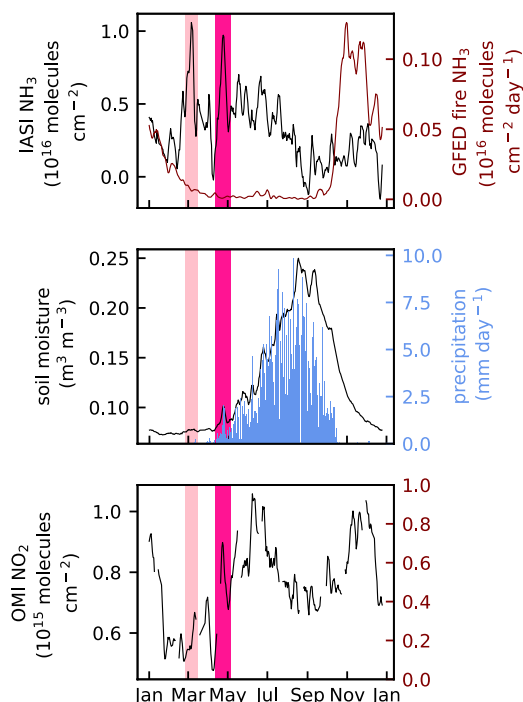
Figure 2: *Early growing season NH₃ pulses temporally associated with changes in soil moisture and with NO₂ pulses over the focal study region in the Sahel during 2008.* Top panel: Daily atmospheric NH₃ concentrations from IASI and NH₃ biomass burning emissions from GFED4s. Middle panel: ESA-CCI soil moisture and TRMM precipitation. Bottom panel: atmospheric NO₂ concentrations from OMI. Putative soil emission pulses in March and April are highlighted in bright and dark pink, respectively. GFED4s emissions were converted from a mass-based to molecule-based flux to allow comparison with the IASI retrievals; note the different scales for the left and right y axes of the top panel.
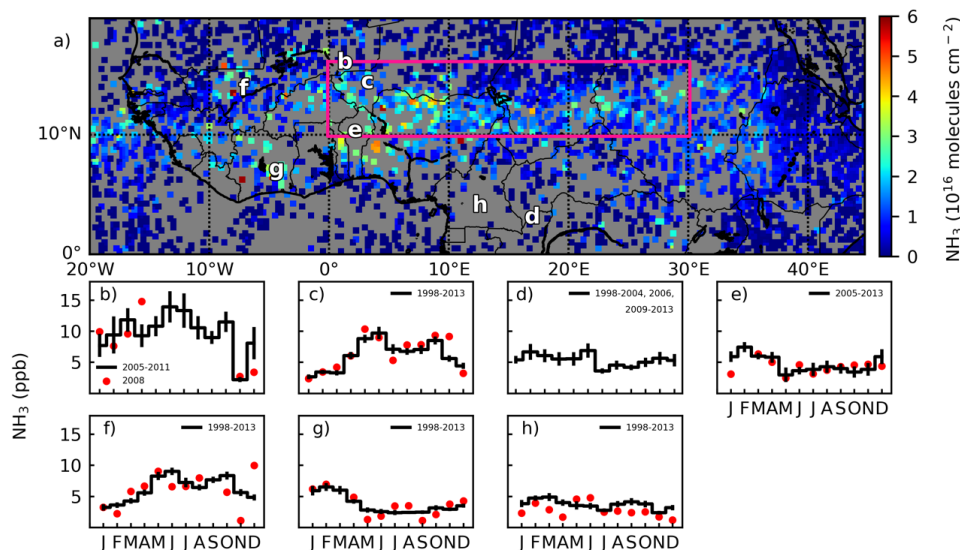
Figure 3. *NH₃ pulsing over the Sahel in April, and geographic variation in the seasonality of surface NH₃ concentrations over north equatorial Africa.* (a) Observations by IASI during April 25 to April 28, 2008 reveal elevated mean atmospheric NH₃ concentrations specifically over the Sahel region (b-h).

5   Monthly NH₃ gas concentrations from sites in the INDAAF network; black lines represent the multi-year mean and standard error for each site, and red dots represent the 2008 value. Data are presented for Agoufou, Mali (b), Banizoumbou, Niger (c), Bomassa, Congo (d), Djougou, Benin (e), Katibougou, Mali (f), Lamto, Côte d'Ivoire (g), and Zoetele, Cameroon (h).
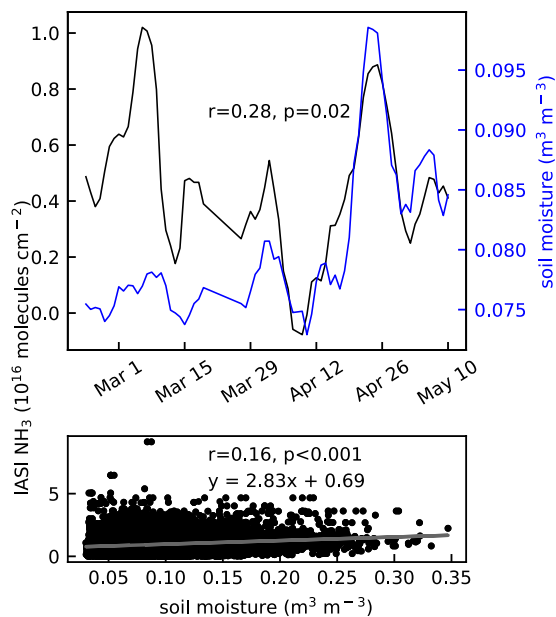
Figure 4. *Correlations between soil moisture and atmospheric NH3 concentrations observed by IASI over the focal study region in the Sahel during the start of the rainy season in 2008.* Top panel: 5-day running mean of daily NH$_3$ concentrations and daily soil moisture for the focal study region from mid-February through the end of April, 2008. Bottom panel: scatterplot of soil moisture versus atmospheric NH$_3$ concentration for each 0.25° pixel in the study region during April, 2008. In both panels, soil moisture data are included only for those 0.25° grid cells where NH$_3$ observations are available for the same day.
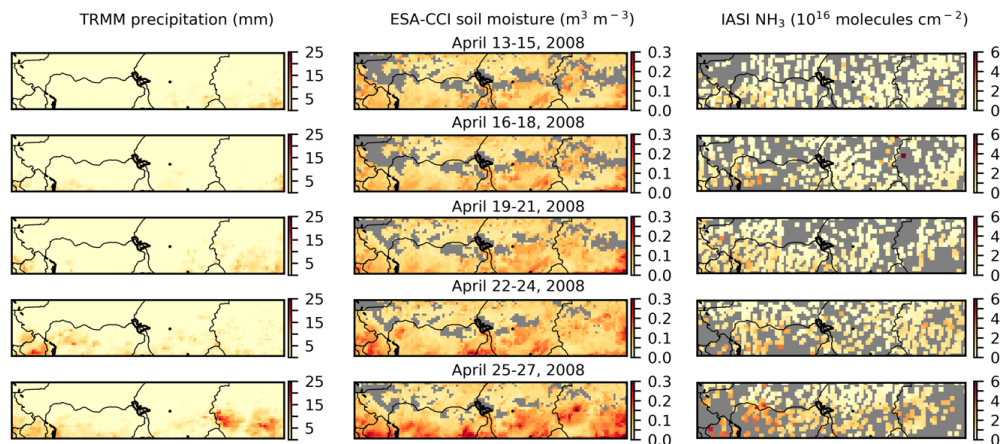
Figure 5. Maps of changing precipitation, soil moisture, and atmospheric NH_3 concentrations for the focal region of the Sahel during the second half of April, 2008. 3-day averages from April 13 through April 27 are presented for precipitation from TRMM (left column), soil moisture from ESA-CCI (middle column) and atmospheric NH_3 concentrations for acceptable retrievals from IASI (right column).
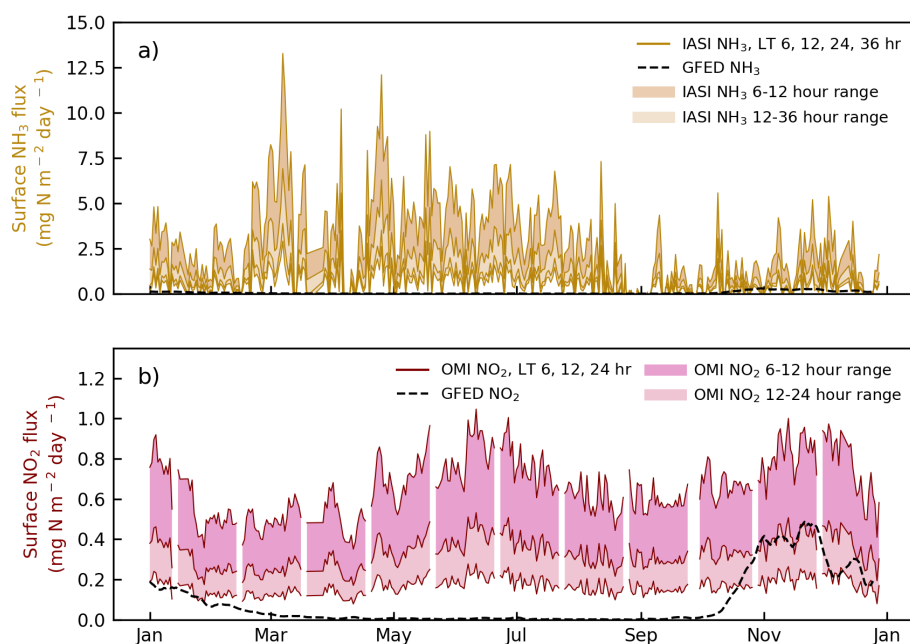
Figure 6. *Comparison of daily total surface fluxes and biomass burning emissions of a) NH₃-N and b)*
NO₂-N for the focal study region in the Sahel during 2008. Total surface fluxes are estimated from
IASI NH₃ and OMI NO₂ observations using a simple box model and assuming effective lifetimes of 12,
24, or 36 hours for NH₃ and of 6, 12, or 24 hours for NO₂. Fire emissions are taken from the GFED4s
database. Note the difference in scales, and that shorter effective lifetimes result in higher modeled
emissions.